Synthesis, Structural Characterizations and Magnetic Properties of a Series of Mono-, Di- and Polynuclear Manganese Pyridinecarboxylate Compounds

Deguang Huang,[a] Wenguo Wang,[a] Xiaofeng Zhang,[a] Changneng Chen,[a] Feng Chen,[a] Qiutian Liu,*[a] Daizheng Liao,[b] Licun Li,[b] and Licheng Sun[c]

Keywords: Carboxylate ligands / Coordination polymers / Magnetic properties / Manganese / X-ray diffraction

Seven new manganese(II, III, IV) pyridinecarboxylate compounds $(Et_4N)[MnCl_2(pic)_2]$ (**1**, Hpic = picolinic acid) $[MnCl(pic)_2(H_2O)]\cdot H_2O$ (**2**), $[MnCl(pic)(H_2O)_2]_n$ (**3**), $[Mn(pic)_2]_n$ (**4**), $[MnCl(pic)]_n$ (**5**), $[MnCl_2(4\text{-}C_5H_4NHCOO)]_n$ (**6**) and $[Mn_2O_2(pic)_4]$ (**7**) were synthesized and structurally characterized. The picolinate ligand coordinates to the Mn ion forming a chelating five-membered ring which constructs diverse architectures by various bridging modes, such as μ-Cl, $\mu_{1,1}$- and $\mu_{1,3}$-carboxylate bridges (*syn-syn* and *syn-anti* modes). The interaction between the pyridyl rings is discussed, displaying a face-to-face π-π stacking for complex **6** and a T-shaped C–H···π attraction for complex **4**. Complex **3** has an infinite zigzag chain structure in which two neighboring Mn ions are linked by a carboxylate bridge in a *syn-anti* mode. In complex **4**, the $Mn(pic)_2$ fragments are joined to each other by double $\mu_{1,1}$-carboxylate bridges, forming a 2D layer structure. Complex **5** contains Mn_4O_4 square subunits which are connected by double μ-Cl bridges to form a grid-like 2D structure. The isonicotinate complex **6** has a zigzag chain structure containing mixed double μ-Cl and $\mu_{1,3}$-carboxylate bridges in a *syn-syn* mode. Protonation at the pyridyl-N position was found and identified by the IR and magnetic properties of **6**. The participation of an oxidizing agent like MnO_4^- leads to complexes containing higher valent manganese (**1**, **2** and **7**). The IR spectra of these complexes are discussed and found to be consistent with the structural features. The magnetic properties of complexes **4**, **5** and **6** have been investigated. Antiferromagnetic coupling interactions were observed and satisfactory fitting results were obtained with *J* values ranging from –0.63 cm^{-1} to –2.35 cm^{-1}. The magnetic parameters of these complexes, together with the parameters of other Mn complexes with comparable structures, are compared and discussed based on the bridging modes.

Introduction

Metal-ligand coordination polymers are attracting increasing attention owing to their potential applications as novel functional materials in catalysis, magnetism, molecular recognition and other fields.[1] Meanwhile, the increasing interest in the coordination chemistry of manganese also stems from the involvement of manganese in several biological redox-active systems,[2,3] especially in the oxygen-evolving complex[4] (OEC) of photosystem II (PS II), which is believed to be a tetranuclear $Mn^{II,III,IV}$ aggregate[5] with O- and N-donors from a carboxylate group and a histidine, respectively.[6] The binding[7] of water to the Mn site and the presence[8] of chloride anion are important structural features of the OEC.

Three isomers of pyridinecarboxylic acid, which contains both O- and N-donors, exhibit remarkable coordination modes to metal ions. Picolinic acid is the most commonly used to obtain metal complexes — its different coordination modes are shown in Scheme 1 — in which a chelating five-membered ring is always found. A number of Mn picolinate complexes with nuclearity[9–12] from 1 to 10 or with a polymeric structure[13] have been reported in the past two decades. However, only a few of these Mn complexes possess a polymeric structure[13] or contain a chloride ligand.[11]

Compared to the coordination modes of the picolinate, there is an obvious difference for 3-, and 4-pyridinecarboxylates, which do not form a chelate ring when they coordinate to metals. Mn complexes[14,15] of these ligands with a polymeric structure are also rare. In order to develop the diversity of the architectures in Mn pyridinecarboxylate chemistry, especially picolinate chemistry, we are interested in the preparation of Mn/pyridinecarboxylate complexes containing a chloride anion, to see what fascinating network topologies are obtained. In this work several Mn com-

[a] State Key Laboratory of Structural Chemistry, Fujian Institute of Research on the Structure of Matter, Chinese Academy of Sciences,
Fuzhou 350002, China
Fax: (internat.) + 86-591-371-4946
E-mail: lqt@ms.fjirsm.ac.cn
[b] Department of Chemistry, Nankai University,
Tianjing 300071, China
[c] State Key Laboratory of Fine Chemicals, Dalian University of Technology,
Dalian, China

  DOI: 10.1002/ejic.200300586

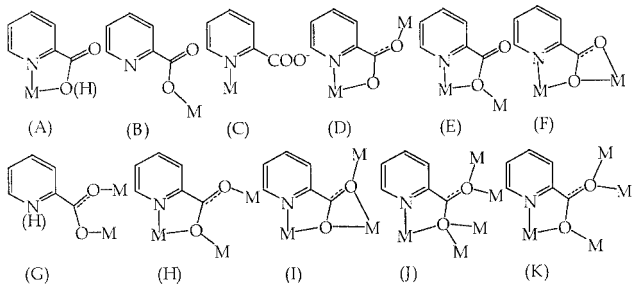

Scheme 1. Possible coordination modes of picolinate to metal ions; modes **A**, **D**, **E**, **H** and **I** have been found in Mn picolinate complexes

plexes with the Mn oxidation states from II to IV are reported, of which four complexes possess a chain-like structure and five contain Mn−Cl ligation.

Results and Discussion

Synthesis

Hundreds of manganese complexes containing Mn−Cl bonds have been reported, of which more than one hundred contain both O- and N-donors from a Schiff base and a nitrogen-containing heterocycle. In this work pyridinecarboxylic acid and $MnCl_2{\cdot}4H_2O$ were used to provide the O- and N-donors and the Cl, respectively. Complexes **1**−**7** were obtained by both conventional solution synthesis and solvothermal methods. Complex **5**, containing an Mn−Cl bond, was obtained in DMF by a solvothermal method, while with a similar molar ratio of reagents and the same reaction temperature to those used for preparing **5** (see Exp. Sect.), complex **4** was synthesized and was found not to contain an Mn−Cl component. This difference is considered to arise from the polarity of the solvents adopted for the syntheses of **4** and **5**. Depending on the polarity of the solvent, DMF or H_2O gives rise to the dissociation of the Mn−Cl bond, leading to the disappearance of the Cl component in complex **4**, while solvents with lower polarity favor the retention of the Mn−Cl bond in **5**. The participation of an oxidizing agent (MnO_4^-) results in the formation of complexes with higher valent manganese. Compounds **1**, **2** and **7** containing Mn^{III} and Mn^{IV} were obtained in the presence of the oxidizing agent or after a prolonged exposure to air. The dinuclear Mn^{IV} compound **7** has been obtained in other laboratories by different methods[10,16] with a difficulty in crystallizability. We have improved the synthesis by reducing the $KMnO_4$:$Mn(OAc)_2$ ratio to avoid the large amount of insoluble precipitates. A co-product, $Mn(pic)_3$, was obtained and isolated, leading to an improved crystallization of complex **7**.

Structure

The structures of mononuclear **1** and **2** are shown in Figure 1 and 2, respectively. Their structures contain an Mn unit together with a counterion for **1** or a solvate molecule for **2**. The Mn atom in both the compounds has a distorted octahedral coordination geometry, whilst Mn1 in complex **1** lies on a crystallographically imposed inversion centre. Both the chelating five-membered rings lie in the equatorial plane, with largest deviations of 0.1067 Å and 0.1447 Å for the constituent atoms of **1** and **2**, respectively. Two terminal *trans*-ligands coordinate to the Mn ion forming linear Cl−Mn−ClA (180° for **1**) and Cl−Mn−O5 [177.60(11)° for **2**] arrays. The Mn−Cl [2.504(1)−2.525(1) Å] and the $Mn-O_{H_2O}$ [2.324(4) Å] bond lengths are obviously lengthened, indicating a Jahn−Teller elongation of high spin d^4 Mn^{III} along the axial direction for the two Mn^{III} complexes. Consequently the $Mn^{III}-Cl$ and $Mn^{III}-O_{H_2O}$ bonds are longer than those found in the Mn^{II} complexes **3**−**6** (Table 1). This Jahn−Teller elongation has previously been observed in other Mn^{III} complexes, in which $Mn^{III}-Cl$ bond lengths of 2.510−2.541 Å were observed.[17] There was still some doubt as to whether the ligand is picolinic acid rather than picolinate. A bond valence sum (BVS) analysis[18] was therefore performed to calculate the oxi-

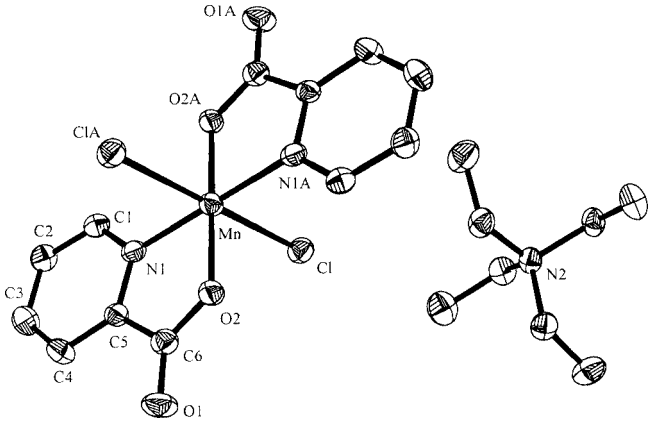

Figure 1. ORTEP representation of compound **1** showing 30% probability displacement ellipsoids and the atom numbering

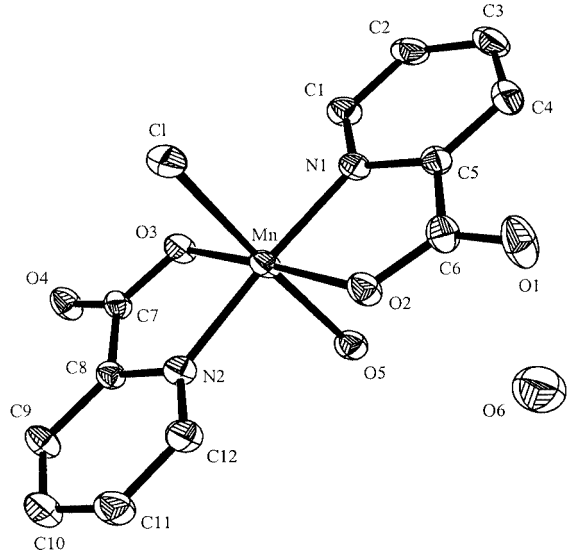

Figure 2. ORTEP representation of compound **2** showing 30% probability displacement ellipsoids and the atom numbering

Table 1. Selected bond lengths (Å) and angles (°) for **1**−**7**

	1	**2**	**3**	**4**	**5**	**6**	**7**
Mn−O	1.903(3)	1.897(4) 1.901(4)	2.173(2) 2.205(2)	2.122(2)−2.232(2)	2.190(2)−2.342(2)	2.1260(18)	1.940(2) 1.918(1)
Mn−N	2.017(3)	2.010(5) 2.015(5)	2.272(3)	2.277(2) 2.297(3)	2.227(2)		2.009(2) 2.050(2)
Mn−Cl	2.525(1)	2.504(1)	2.4914(9)		2.501(1) 2.500(1)	2.570(1) 2.595(1)	
$Mn-O_{H_2O}$		2.324(4)	2.175(3) 2.181(3)				
$Mn-O_{oxo}$							1.809(1) 1.804(1)
Mn···Mn				3.507	4.425 3.637	3.621	2.701(1)
N−Mn−N	180	175.52(14)		115.63(10)			166.91(9) 94.26(9)
Cl−Mn−Cl	180				87.63(2)	180 82.77(3)−97.23(3)	
O−Mn−O	180	87.12(13)−87.49(13) 174.56(14)	81.44(7)−90.72(9) 178.51(8)	74.00(8)−113.17(8) 160.00(9)	57.33(5)−88.21(8)	180	83.08(9)−96.23(7) 164.82(9)−171.97(6)
O−Mn−N	82.55(13) 97.45(13)	82.54(13)−97.63(14)	72.99(7)−89.61(8) 154.43(8)	71.63(8)−97.55(9) 145.34(8)−155.06(9)	74.41(6)−100.44(6) 151.53(7)		80.61(6)−97.23(7) 173.56(6)
O−Mn−Cl	90.17(9) 89.83(9)	92.42(10)−93.00(10) 177.15(10)	89.46(6)−111.25(6) 167.30(5)		90.87(4)−104.91(5) 161.65(4)−172.24(4)	87.83(5)−92.17(5)	
N−Mn−Cl	86.98(10) 93.02(10)	90.96(11)−93.50(11)	94.32(6)		98.20(5)−97.87(5)		
Mn−Cl−Mn					91.59(2)	89.03(3)	
Mn−O−Mn				106.00(8)	155.00(7)		96.77(7)

dation state of the metal centre. The bond valences (s) were calculated according to Equation (1), where r is the observed bond length and r_0 and B are empirically determined parameters.[18]

$$s = exp[(r_0 - r)/B] \quad (1)$$

This BVS analysis did not support an Mn^{2+} oxidation state. X-band EPR spectra were recorded on a Bruker-ER420 spectrometer for complexes **1** and **2** as solid samples. No signals were observed, which could be an indication of the Mn^{III} ion since the EPR signal is very difficult to observe with traditional perpendicular polarization EPR spectroscopy at X-band for the spin $S = 2$ Mn^{III} ion. An obvious difference between **1** and **2** is that the terminal water ligand gives rise to extended hydrogen bonding interactions between neighboring molecules of **2**, such as O5···Cl [3.272(5) Å] and $O5\cdots O_{carboxyl}$ [2.736(5) and 2.873(6) Å], giving a one-dimensional chain structure. In contrast, the structure of complex **1**, with two chloride ligands, contains only the discrete ions.

Compound **3** has an infinite zigzag chain structure in which the Mn ions are linked to each other by $\mu_{1,3}$-OCO bridges in a *syn-anti* mode, as shown in Figure 3. The Mn ion is located at the center of a distorted octahedron and the picolinate chelate ring forms the equatorial plane together with Cl and the symmetrically related O1A atoms. All the bond lengths [2.170(2), 2.171(2), 2.176(2) and 2.209(2) Å for Mn−O; 2.275(2) Å for Mn−N; 2.492(1) Å for Mn−Cl] were used for the BVS analysis.[18] The BVS of Mn was calculated to be 2.097 by summing the values of *s*, which supports the oxidation state of the Mn^{II} ion. Interestingly, except for the O3 and O4 atoms, which lie in the axial direction, all the other atoms are coplanar, with the largest deviation from the least-squares plane being 0.0197 Å. Consequently, the zigzag chain contains all the atoms in the common plane except for the axial atoms. The O3−Mn−O4 axis [178.51(8)°] is perpendicular to the plane, with bond angles (O3−Mn−X and O4−Mn−X, X = N, O, Cl) ranging from 89.21(7)° to 90.49(11)°. Figure 4 shows a packing diagram of the compound, in which hydrogen bonding interactions of the type $O_{carboxylate}\cdots H-O_{aqua}$ [2.830(3) and 2.821(3) Å] and $Cl\cdots H-O_{aqua}$ [3.144(2) and 3.153(2) Å] link the neighboring parallel zigzag chains, constructing a two-dimensional double-layer network. Rectangular channels are observed in the polymeric structure, with dimensions of 3.22 × 4.16 Å. However, these channel dimensions are measured between atom centers. In a space-filling plot (Figure 4B) taking into account the van der Waals radii, there is only a small channel left. It should also be pointed out that no π-π stacking is observed between the pyridyl rings since their separation is too large (> 3.8 Å)[19] for a van der Waals interaction; the pyridyl rings are found in a parallel and face-to-face alignment.

The structure of compound **4** is shown in Figure 5. The BVS of the central Mn ion is calculated[18] to be 2.028, indicating an Mn^{II} oxidation state and the ligand to be a picolinate anion. In the $Mn(pic)_2$ fragment, the two chelating five-membered rings are nearly perpendicular to each other,

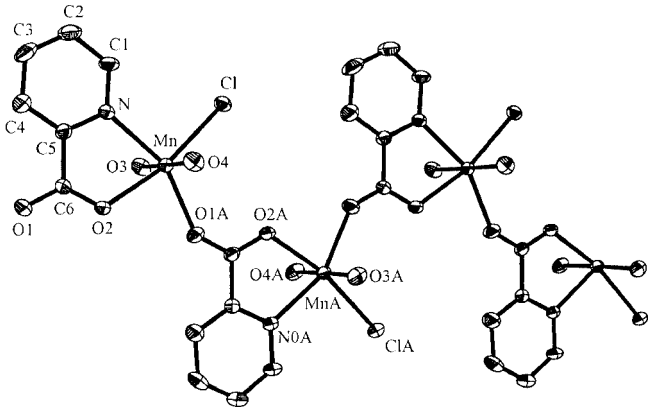

Figure 3. ORTEP representation of compound **3** showing 30% probability displacement ellipsoids and the atom numbering

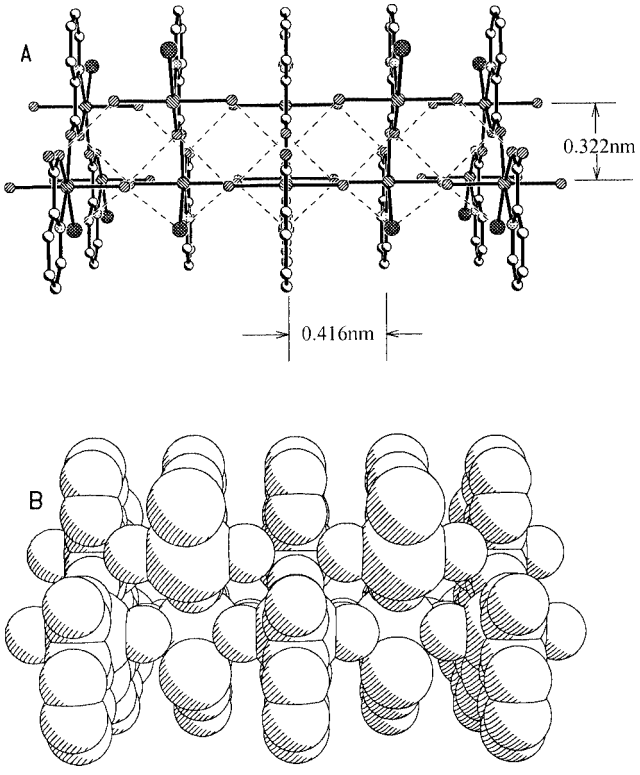

Figure 4. Packing diagram (A) of **3** showing the rectangular channels; hydrogen bonding interactions are shown by dotted lines; (B) space-filling plot to show the small channel space

with a dihedral angle of 85.2°. These fragments are linked pairwise by double μ-$O_{carboxylate}$ bridges to form [Mn_2(pic)$_4$] subunits, with an Mn···Mn distance of 3.507 Å. All the bond angles around the Mn ion range from 145.34(8)° to 160.00(9)° for *trans* angles and from 71.63(8)° to 115.63(10)° for the others, indicating a seriously distorted octahedral geometry. The picolinate anions link the Mn^{II} ions through a $\mu_{1,3}$-OCO bridge in a *syn-anti* mode together with an η^1-monodentate mode to construct a two-dimensional layer structure, as shown in Figure 6, in which π-π stacking has not been observed owing to the large separation between the parallel displaced pyridyl rings. However, a point-to-face (T-shape) interaction — a C−H···π attraction[19] — appears to exist between the pyridyl rings that are perpendicular to each other with a separation of 3.7 Å (Figure 6). An isostructural 2-pyrazinecarboxylate Mn^{II} complex[20] has been reported to have almost the same crystallographic data to that of **4**.

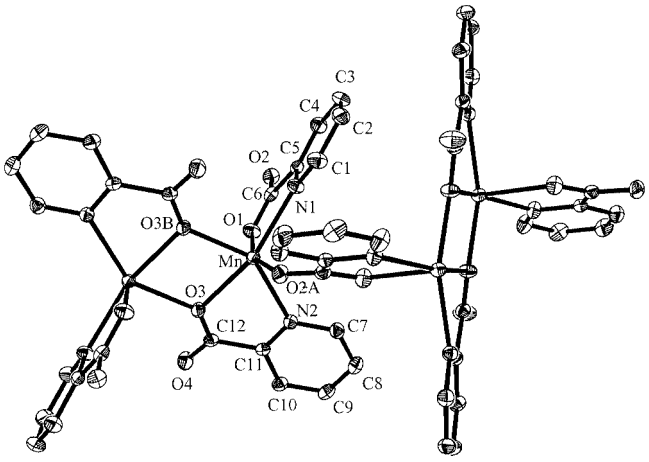

Figure 5. ORTEP representation of compound **4** showing 30% probability displacement ellipsoids and the atom numbering.

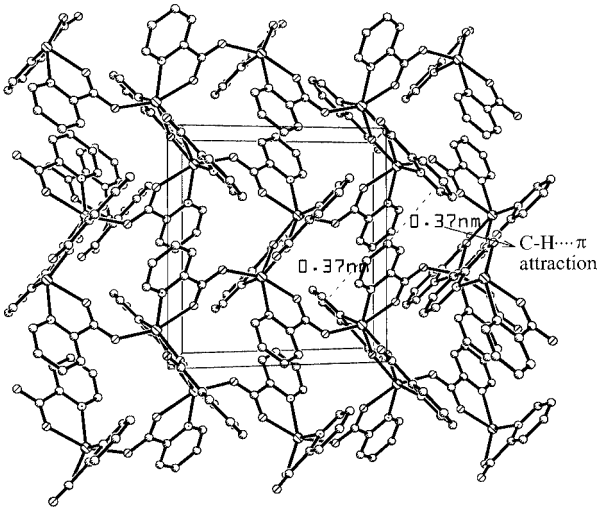

Figure 6. The 2D layer structure of compound **4** along the *a* axis

Complex **5** contains the simplest unit [Mn(pic)Cl], where the picolinate coordinates to the Mn center according to the coordination mode F (Scheme 1) to link two neighboring Mn atoms in the space group $P4_2/n$. The fragments combine, leading to a tetra-manganese [Mn_4(pic)$_4$] subunit, which has an alternating [Mn−O]$_4$ eight-membered ring that looks like a distorted square, as shown in Figure 7, with an Mn···Mn separation of 4.425 Å for each Mn···Mn edge and an O−Mn−O angle of 88.3°. The Mn−O [2.190(2), 2.342(2) and 2.232(2) Å], Mn−N [2.227(2) Å] and Mn−Cl [2.500(1), 2.501(1) Å] bond lengths were used for the BVS calculation[18] and the sum of the values of *s* is 1.98, indicating the Mn^{II} oxidation state. Two kinds of carboxylate bridges of the picolinate anion — a $\mu_{1,1}$-OCO

bridge and a $\mu_{1,3}$-OCO bridge in a *syn-anti* mode — link simultaneously the Mn ions to form five- and four-membered chelating rings by O,N- and O,O-donors. A small dihedral angle of 4.0° for the two chelating rings indicates an approximate coplanarity of the picolinate ligand and the two Mn ions, as shown in Figure 7. Around the $[Mn-O]_4$ square, the neighbouring picolinates are perpendicular to each other with a dihedral angle of 89.0°, while the opposite ones are approximately parallel, with a dihedral angle of 11.9°.

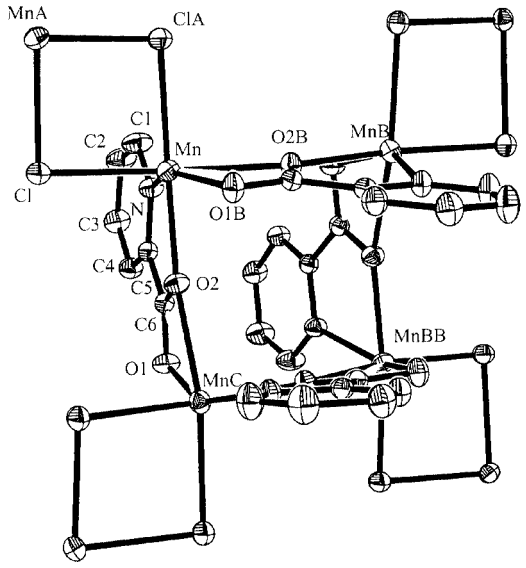

Figure 7. The unit structure of compound **5** showing 30% probability displacement ellipsoids and the atom numbering; a tetramanganese subunit $[Mn(pic)]_4$ is presented

The above $[Mn-O]_4$ squares are connected by double μ-Cl bridges forming the second type of $[Mn(\mu_2\text{-}Cl)_2Mn]$ square-like units, with an Mn−Cl distance of 2.501 Å and angles of 87.6−91.6°. An isostructural Cu analogue $[CuCl(pic)]_n$ has been reported to have similar metal-ligand square-like units.[21] The two types of squares are alternately linked by sharing the Mn ions to form a 2-D Mn_nCl_n quasi-planar grid-like sheet (Figure 8), while the picolinate planes protrude perpendicularly on both sides of the sheet. From the packing diagram (Figure 9), it can clearly be noticed that these salients interpenetrate to give a tightly packed structure without any hydrogen-bonding interactions.

The structure of the isonicotinate complex **6** is composed of a one-dimensional $[Mn(\mu\text{-}C_5H_4NHCOO)(\mu\text{-}Cl)_2]_n$ chain; the $Mn(C_5H_4NHCOO)Cl_2$ unit is shown in Figure 10. A carboxylate bridge in a *syn-syn* mode and double μ-Cl bridges exist between neighboring Mn ions. This is a novel coordination mode for Mn isonicotinate complexes. This is also the first example of a metal complex that contains mixed double Cl and single $\mu_{1,3}$-OCO bridges, the only similar bridging mode was found in $\{Hg_3(L)Cl_6\}_n$ [22] [L = 2,5-bis(pyridino)adipate] containing mixed single Cl and single $\mu_{1,3}$-OCO bridges. In addition, protonation at the pyridyl-N atom was found and was identified by IR spectroscopy (vide infra). A similar proton shift has been observed in a

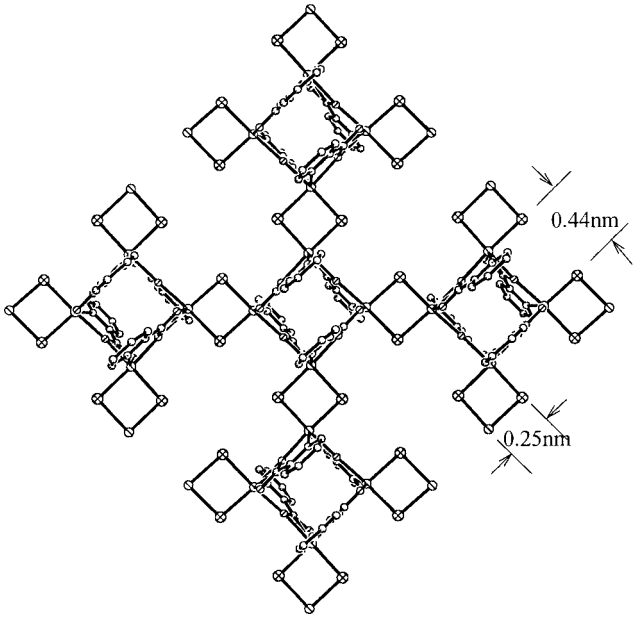

Figure 8. The 2D layer structure of **5** along the *c* axis

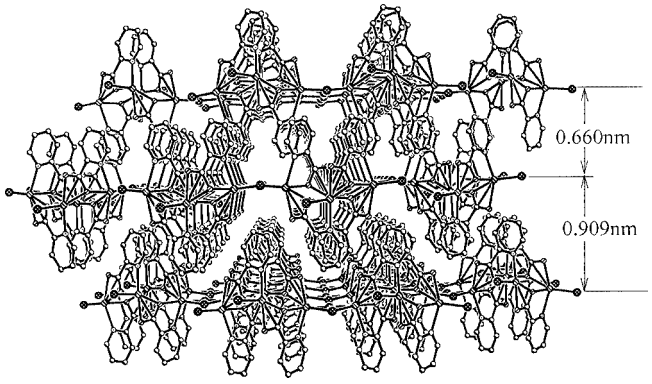

Figure 9. Packing diagram of **5** along the *a* axis showing the inlaid layer structure

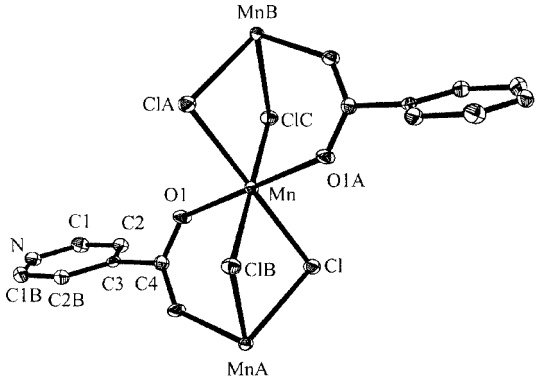

Figure 10. ORTEP representation of compound **6** showing 30% probability displacement ellipsoids and the atom numbering

few metal isonicotinate complexes.[23] The ESR spectra of **6** were recorded on a Bruker-ER420 spectrometer at X-band at room temperature and at 77 K as solid samples, showing strong signals at $g = 2$ and implying the existence of Mn^{II}

species with spin $S = 5/2$. A BVS calculation[18] for the Mn ion gives the sum of the *s* values to be 1.99, confirming the Mn^{II} oxidation state. The Mn^{II} ion lies at a centre of symmetry, forming a slightly distorted octahedron with O−Mn−Cl angles ranging from 87.83(5)° to 92.17(5)°. Parallel pyridine rings are alternately insert between the neighboring zigzag chains (Figure 11) with a ring separation of 3.621 Å that is slightly larger than the sum of the van der Waals contact radii (3.4 Å) for two C atoms, showing a face-to-face π-π stacking interaction. Owing to the restriction by this arrangement, the pyridine rings cannot be coplanar with the carboxylic group, and the dihedral angle was observed to be 67.2° between the carboxylate group and the pyridyl ring. Hydrogen-bonding interactions (N−H···Cl) exist between the neighboring chains to construct a 2D layer structure.

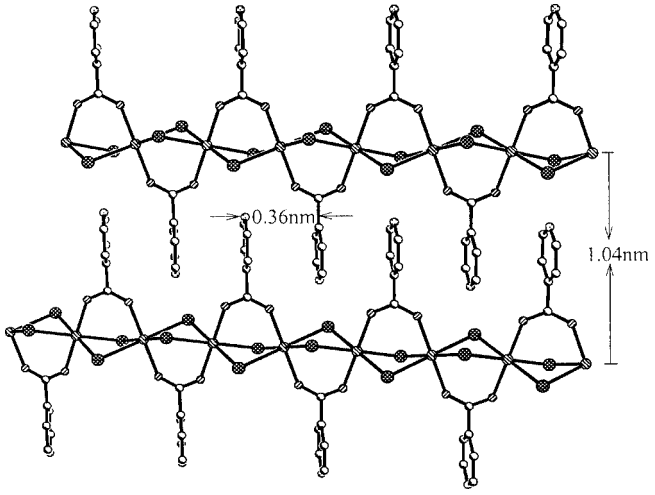

Figure 11. The 1D zigzag chain of complex **6**

Compound **7** contains Mn ions and double oxo-bridges as well as the picolinate ligands. It should be pointed out that the first such complex $[Mn_2O_2(pic)_4]\cdot CH_3CN$ was reported by Christou.[10] Similar structural parameters to those of $[Mn_2O_2(pic)_4]\cdot CH_3CN$, and the BVS of 4.1,[18] indicate that the Mn atom is definitely tetravalent in **7**. An interesting difference between both structures is the lower symmetry of **7** than that of $[Mn_2O_2(pic)_4]\cdot CH_3CN$. The structure of **7** is shown in Figure 12. A twofold axis passes through the Mn1 and Mn2 ions with an Mn−Mn bond length of 2.701(1) Å. Both the octahedral Mn ions coordinate differently to the picolinate ligands. Two nitrogen atoms are located in the *trans*-positions for the Mn1 ion, with an N1−Mn1−N1′ angle of 166.91(9)°, while they are in the *cis*-positions for Mn2, with an N2−Mn2−N2′ angle of 94.26(9)°. A similar situation is also observed for the carboxylate oxygen atoms: O1−Mn1−O1′ of 92.37(10)° and O4−Mn2−O4′ of 164.82(9)°. This is an important difference between **7** and $[Mn_2O_2(pic)_4]\cdot CH_3CN$, as in the latter both N atoms are axially arranged in the octahedron of any Mn ion.

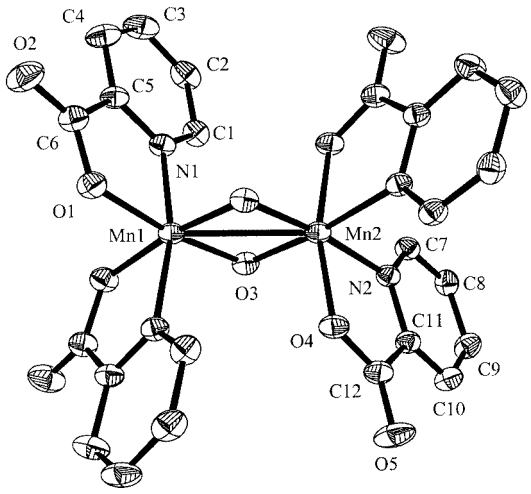

Figure 12. ORTEP representation of **7** showing 30% probability displacement ellipsoids and the atom numbering; Mn···Mn distance 2.701 Å

IR Spectroscopy

In agreement with previously published data,[9,10] the IR spectra of the Mn picolinate complexes (**1**−**5** and **7**) in the 400−4000 cm^{-1} region only exhibit signals related to the picolinate ligand, for example 1649, 1309, 1049 and 764 cm^{-1} for **1**; similar signals are found for the other complexes. The signals in the range from 1610 cm^{-1} to 1682 cm^{-1} can be assigned to the asymmetric stretching vibrations for the COO^- groups, and the signals between 1446 and 1497 cm^{-1} correspond to the symmetric stretching vibrations $\nu_s(COO^-)$. The isonicotinate signals for complex **6** are also similar to those reported previously.[15] The carboxylate in **6** exhibits similar asymmetric and symmetric stretching vibrations to those of other picolinate complexes. The N−H stretching frequency is observed at 3217 cm^{-1}, suggesting[24] protonation at the nitrogen atom of the pyridyl. Complexes **1** and **7** contain the carboxylate groups in unidentate coordination mode, and the separation (Δ) between $\nu_{as}(COO^-)$ and $\nu_s(COO^-)$ is 209 cm^{-1}, which is consistent with the generally accepted value[25] ($\Delta > 200$ cm^{-1}) for a unidentate-coordinated carboxylate, while complexes **5** and **6** give a separation value of less than 200 cm^{-1}, which is considered to correlate to a chelating carboxylate in **5** ($\Delta = 135-164$ cm^{-1}) or a bridging bidentate ligand in a *syn-syn* configuration in **6** ($\Delta = 174-197$ cm^{-1}). The strong and broad band centered at 3385 cm^{-1} for **3** is assigned to the H−O−H stretching vibration of the water ligand on the basis of the known structure. Medium-intensity absorptions are observed in the range from 3080 to 3120 cm^{-1} and can be attributed to the δ(CH) of the pyridyl.

Magnetic Properties

The magnetic properties of Mn complexes are often important. Complexes **1** and **2**, however, are mononuclear, and complex **3** has an Mn···Mn separation too large to permit magnetic exchange, while the magnetic properties have already been reported for $[Mn_2O_2(pic)_4]\cdot CH_3CN$.[10] There-

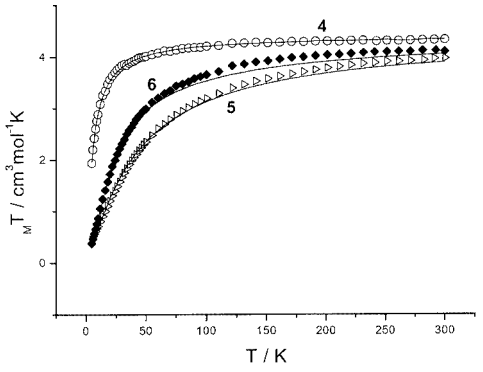

Figure 13. Thermal variations of the $\chi_M T$ product for **4** (circle), **5** (triangle) and **6** (square); the solid lines represent the best-fit curves

fore we report here the magnetic behavior of complexes **4**, **5** and **6**. Figure 13 shows the temperature dependence of the product ($\chi_M T$) of molar susceptibility and the temperature for the three complexes. For **4**, the value of μ_{eff} at 300 K amounts to 5.88 μ_B, close to the spin-only value of 5.92 μ_B for $S = 5/2$. For **5**, the value of μ_{eff} at 300 K amounts to 5.63 μ_B which is slightly lower than the spin-only value for $S = 5/2$. The effective magnetic moment smoothly decreases with a decrease of the temperature, indicating an antiferromagnetic interaction between neighboring magnetic species for both the complexes. Figure 6 and 8 show the 2D layer structures of **4** and **5**, which contain the [$Mn_2(\mu\text{-}O_{carboxylate})_2$] and [Mn2($\mu_{1,3}$-OCO)] moieties for **4**, and the [$Mn_2(\mu\text{-}Cl)_2$] and $Mn-O_{carboxylate}-Mn$ moieties for **5**. These moieties are arranged alternately to construct alternating chains along two directions, therefore an alternating chain with a classical spin S_{eff} is suggested as a model to analyze the magnetic data for both complexes (Scheme 2). The susceptibilities of the chains are obtained from Equation (2), which was deduced by Rojo[26] and is suitable for the fitting of an alternating chain model.

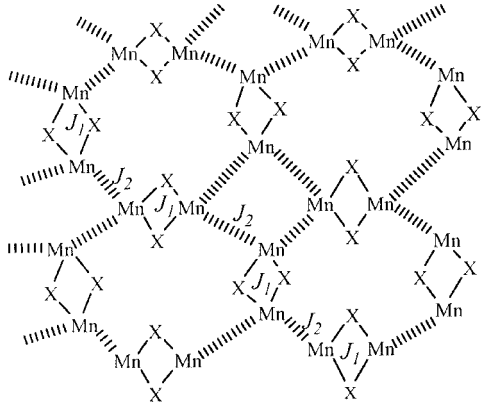

4: X = $O_{carboxylate}$ ⫶⫶⫶⫶⫶ = $\mu_{1,3}$–OCO

5: X = Cl ⫶⫶⫶⫶⫶ = μ–$O_{carboxylate}$

Scheme 2. An alternating chain ($J_1 - J_2$) with a classical spin S_{eff} is shown; the interactions between the S_{eff} chains are treated further according to a uniform chain

$$\chi_{chain} = \frac{Ng'^2\beta^2}{3kT}\left(\frac{1+u_1+u_2+u_1u_2}{1-u_1u_2}\right)$$

$$\text{where} \quad u_1 = Coth\left(\frac{J_1}{kT}\right) \qquad u_2 = Coth\left(\frac{J_2}{kT}\right) - \frac{kT}{J_2} \tag{2}$$

$$J_1 = J_1 S(S+1) \qquad g' = g[S(S+1)]^{1/2}$$

The magnetic interactions between the chains are treated based on the assumption that the alternating chain can be seen as an entity with classical spin S_{eff}. The S_{eff} should obey the Curie expressions [Equation (3)].

$$S_{eff}(S_{eff}+1) = 3k(\chi_{chain}T)/Ng^2\beta^2 \tag{3}$$

These S_{eff} entities are connected by $\mu_{1,3}$- or $\mu_{1,1}$-carboxylate bridges and can be treated as a uniform chain. Consequently, the magnetic susceptibilities of the systems can be calculated by Equation (4) for a classical chain.[27]

$$\chi_M = [Ng^2\beta^2 S_{eff}(S_{eff}+1)/3kT](1+u)/(1-u)$$

$$\text{where} \quad u = Coth[J_2 S_{eff}(S_{eff}+1)/kT] - kT/J_2 S_{eff}(S_{eff}+1) \tag{4}$$

The least-squares fitting results of the experimental data are: $g = 2.02$, $J_1 = -0.63$ cm^{-1}, $J_2 = -0.14$ cm^{-1} and $R = 4.63 \times 10^{-5}$ for **4**, and $g = 2.00$, $J_1 = -0.6$ cm^{-1}, $J_2 = -2.7$ cm^{-1} and $R = 4.92 \times 10^{-4}$ for **5**, where $R = \Sigma[(\chi_M)^{cal} - (\chi_M)^{obs}]^2/[(\chi_M)^{obs}]^2$.

The μ_{eff} value at 300 K for **6** amounts to 5.72 μ_B, close to the spin-only value of 5.92 μ_B for Mn^{II} with $S = 5/2$, supporting the protonation of the nitrogen atom in $C_5H_4N^+HCOO^-$. A uniform Mn chain model [Mn(μ-Cl)$_2$($\mu_{1,3}$-OCO)]$_n$ was used to fit the magnetic data of **6** and the magnetic susceptibility was calculated by Equation (5) for a uniform chain:[28]

$$\chi_M = \left(\frac{Ng^2\beta^2}{kT}\right)[A + Bx^2][1 + Cx + Dx^3]^{-1} \tag{5}$$

where $x = |J|/kT$, $A = 2.9167$, $B = 208.04$, $C = 15.543$ and $D = 2707.2$. These coefficients for magnetic susceptibility expressions for Heisenberg chains with $S = 5/2$ have beenused previously.[28] The least-squares fitting leads to $g = 2.00$, $J = -1.1$ cm^{-1} and $R = 2.4 \times 10^{-5}$.

Table 2 lists the magnetic parameters for the three complexes together with the parameters of other Mn complexes with similar structures. Complex **7**, containing the $Mn_2(\mu\text{-}O_{oxo})_2$ unit, shows the largest $|J|$ value among all the complexes in Table 2, which is believed to be correlated to the strong $Mn^{IV}-Mn^{IV}$ bonding interaction. Magnetically active chloride-bridged systems have been reported previously. Complexes containing an $Mn_2(\mu\text{-}Cl)_2$ unit reveal the exchange interactions via double μ-Cl bridges in the range $|J| = 0.2-16$ cm^{-1}, as shown in Table 2. The angular de-

Table 2. Magnetic parameters for Mn complexes with μ-Cl, μ-O and $\mu_{1,3}$-OCO bridges

Complex	*g*	$Mn(\mu\text{-}Cl)_2Mn$				Mn−O−Mn				Ref.
		Mn···Mn (Å)	Mn−Cl−Mn (°)	$J_{Cl,OCO}$[a] (cm^{-1})	J_{Cl}[b] (cm^{-1})	Mn···Mn (Å)	Mn−O−Mn (°)	J_O (cm^{-1})	J_{OCO}[c] (cm^{-1})	
4	2.02					3.507	106.00(8)	−0.63	−0.14	[d]
5	2.00	3.585	91.59(2)		−1.81	4.425	155.00(7)	−2.35		[d]
6	2.00	3.637	89.03(3)	−1.1						[d]
A[e]	1.936					3.503	106.75	−0.48	−0.15	[20]
B[e]	2.02	3.515	90.2		−4.8					[29]
C[e]	2.05	3.344	86.37(2) 88.13(2)		−15.6					[30]
D[e]	2	4.05	98.6(1) 99.5 (1)		0.2					[31]
E[e]	2.02	3.664	93.36(2)		0.42					[32]
F[e]	2.00					4.41	151.0(1)	−1.42		[33]
7·MeCN	1.83					2.747(2)	98.1(2)	−86.5		[10]

[a] Magnetic exchange interaction through μ-Cl and $\mu_{1,3}$-OCO mixed bridges. [b] Magnetic exchange interaction through single atom μ-Cl or μ-O bridge. [c] Magnetic exchange interaction through $\mu_{1,3}$-OCO bridge. [d] This work. [e] **A**: $[Mn(pyz)_2]n$, pyz = 2-pyrazinecarboxylate. **B**: $[MnCl(MeCp)(PEt_3)]_2$. **C**: $[ppn]_2[Mn_2Cl_6]$. **D**: $[Mn(H_2dapd)C1_2]n$, H_2dapd = 2,6-diacetylpyridine dioxime. **E**: $[MnCl(pyz)(H_2O)]n$, **F**: $[\{Mn(bic)(H_2O)\}_2{\cdot}2Br]n$ (bic = bicinate).

pendence of the strength and nature of the magnetic coupling in M(μ-X)M systems has been studied in detail for Cu^{II}_2 and Cr^{III}_2 systems.[34] The Mn−Cl−Mn angle obviously plays an important role in determining the nature and strength of the chloride-mediated coupling. Complexes **5**, **6** and $[MnCl(MeCp)(PEt_3)]_2$ (**B**) have Mn−Cl−Mn angles very close to 90° in their $Mn_2(\mu\text{-}Cl)_2$ units and exhibit an antiferromagnetic coupling, while complexes **D** and **E** have angles larger than 90° and have weak ferromagnetic interactions. It seems that a smaller separation of the Mn^{II} ions (and/or smaller Mn−Cl−Mn angle) results in a larger $|J|$ value, implying that greater overlap between the magnetic orbitals in the $Mn_2(\mu\text{-}Cl)_2$ unit favors the antiferromagnetic exchange of the paramagnetic sites. Complexes **4** and $[Mn(pyz)_2]_n$ (**A**, pyz = 2-pyrazinecarboxylate), which are isostructural, both have an $Mn_2(\mu\text{-}O_{carboxylate})_2$ unit in their structures and exhibit a weak antiferromagnetic coupling. It should also be noted that magnetic coupling through a $\mu_{1,3}$-carboxylate bridge is dependent on the coordination mode of the carboxylate to the paramagnetic centers. There is an efficient overlap between the 3d magnetic orbital of the Mn^{2+} center and the 2p magnetic orbital of the carboxylate group in the order *syn-syn* > *anti-anti* > *syn-anti*.[35] Complexes **4** and **A** have the $\mu_{1,3}$-carboxylate bridges in a *syn-anti* mode, and are therefore less capable of transmitting magnetic interactions ($J_{\mu\text{-}OCO}$ = −0.14 cm^{-1}) than complex **6**, with the carboxylate in a *syn-syn* mode and double Cl bridges. In our work, the transfer pathway via a single-atom (O or Cl) bridge seems to be better than via a $\mu_{1,3}$-carboxylate bridge, $|J_{\mu\text{-}O}|$ or $|J_{\mu\text{-}Cl}| > |J_{\mu\text{-}OCO}|$. However, this is not general since exceptions have been reported by Nagata.[36] A larger $|J_{\mu\text{-}O}|$ value (−2.35 cm^{-1}) was observed for complex **5**, in spite of the larger Mn···Mn separation (4.425 Å). The only comparable complex is $[\{Mn(bic)(H_2O)\}_2{\cdot}2Br]_n$ [bic = bicinate = *N,N*-bis(2-hydroxyethyl)glycinate],[33] in which an Mn···Mn separation of 4.41 Å and Mn−O−Mn angle of 151° were found. It is thought that a linear Mn−O−Mn array may lead to an efficient overlap of the magnetic orbitals between the 3d magnetic orbitals of the Mn^{2+} and the 2p magnetic orbitals of the carboxylic oxygen atom. Consequently, complex **5** has a $|J_{\mu\text{-}O}|$ value larger than that of **4**. However, additional examples are required before such arguments can be considered valid.

Conclusion

Six new manganese picolinate or isonicotinate complexes were synthesized and structurally characterized. The chelating five-membered rings of the Mn picolinate construct diverse architectures, such as the zigzag chain of **3**, the 2D layer structure of **4** or the grid-like 2D structure of **5**, by $\mu_{1,3}$-OCO bridges in a *syn-anti* mode, and $\mu_{1,1}$-carboxylate or μ-Cl bridges, respectively. The isonicotinate complex **6** contains $MnCl_2(4\text{-}C_5H_4NHCOO)$ units which form an infinite zigzag chain by double μ-Cl and $\mu_{1,3}$-OCO bridges in a *syn-syn* mode.

In the syntheses of these complexes, the participation of an oxidizing agent leads to complexes with higher-valent manganese (III or IV for **1**, **2** and **7**). The removability of the chloride anion depends on the polarity of the solvent. Strongly polar DMF or H_2O allow the dissociation of the Mn−Cl bond, while other solvents favor the retention of the Mn−Cl bond in the products. This removability may be related to the doubts over whether the Cl^- ion is a ligand of the Mn site in OEC. We have assumed that the Cl^- ion is removable outside or inside the coordination sphere of the Mn ions.[37]

The IR spectra were discussed and various separations [$\Delta = \nu_{as}(COO) - \nu_s(COO)$] were obtained for these complexes, indicating unidentate, bidentate bridging or chelating coordination modes for the carboxylate groups. This is consistent with the structural features of the complexes. The

N−H stretching frequency at 3217 cm^{-1} supports the structural analysis for complex **6**, with protonation at the nitrogen atom of the pyridyl unit.

Complexes **4**, **5** and **6** exhibit antiferromagnetic coupling interactions with J values ranging from -0.63 cm^{-1} to -2.35 cm^{-1}. Comparison of the magnetic parameters with those of other Mn complexes with comparable structures indicates the angular dependence of the strength and the nature of the magnetic coupling in M(μ-Cl)M systems: a smaller Mn−Cl−Mn angle results in a larger $|J|$ value.

Experimental Section

General: All manipulations were performed under aerobic conditions, and all commercially available reagents were used as received, except for the complex Et_4NMnO_4 which was prepared according to a literature procedure.[38] IR spectra were recorded on a Magna-75 FT-IR spectrophotometer as KBr pellets. The variable-temperature susceptibility was measured on a model CF-1 superconducting magnetometer with crystalline sample kept in a capsule at 5−300 K. Diamagnetic corrections were made with Pascal's constants for all the constituent atoms of the complexes determined. Elemental analyses were performed with an Elemental Analyzer Vario EL III.

$(Et_4N)[MnCl_2(pic)_2]$ (1): Tetraethylammonium hydroxide (25% in methanol; 0.5 mL) was added to a solution of picolinic acid (0.123 g, 1 mmol) in 10 mL of CH_2Cl_2/MeCN (1:1, v/v). The solution was stirred for 15 minutes and then $MnCl_2{\cdot}4H_2O$ (0.198 g, 1 mmol) was added. The reaction solution was refluxed for 18 h. After filtration, the filtrate was allowed to stand for one month at room temperature to deposit light-red crystals, which were collected, affording 0.068 g of complex **1**. Yield: 27% based on Hpic. $C_{20}H_{28}Cl_2MnN_3O_4$ (500.29): calcd. C 48.02, H 5.64, N 8.40, Mn 10.98; found C 48.48, H 5.72, N 8.73, Mn 11.05. IR (KBr): $\tilde{\nu}$ = 3080 (w) cm^{-1}, 2987 (w), 2922 (w), 1682 (vs), 1645 (m), 1606 (s), 1497 (m), 1473 (m), 1309 (s), 1275 (s), 1257 (s), 1236 (m), 1142 (s), 1049 (m), 764 (s).

$[MnCl(pic)_2(H_2O)]{\cdot}H_2O$ (2): $MnCl_2{\cdot}4H_2O$ (0.198 g, 1 mmol) was added to a solution of picolinic acid (0.123 g, 1 mmol) in 25 mL of CH_3OH and the solution was stirred for 30 minutes. Then, Et_4NMnO_4 (0.062 g, 0.25 mmol) was added in small portions to the reaction solution to give a dark-red solution. The mixture was filtered and the filtrate was evaporated at room temperature to yield green crystals, which were collected to afford 0.019 g of complex **2** with a yield of 10% based on Hpic. $C_{12}H_{12}ClMnN_2O_6$ (370.63): calcd. C 38.89, H 3.26, N 7.56, Mn 14.82; found C 39.97, H 3.31, N 7.66, Mn 14.90.

$[MnCl(pic)(H_2O)_2]_n$ (3): $MnCl_2{\cdot}4H_2O$ (0.594 g, 3 mmol) was added to a solution of picolinic acid (0.185 g, 1.5 mmol) in 40 mL of CH_3OH/CH_2Cl_2/MeCN (1:1:2, v/v/v) and the solution was refluxed for 24 h. After filtration light red crystals deposited from the filtrate at room temperature. The crystals were collected, affording 0.075 g of complex **3** with a yield of 20% based on Hpic. $C_6H_8ClMnNO_4$ (248.52): calcd. C 29.00, H 3.24, N 5.64, Mn 22.11; found C 29.28, H 3.27, N 5.77, Mn 22.24. IR (KBr): $\tilde{\nu}$ = 3385 (s) cm^{-1}, 3086 (w), 1610 (s), 1587 (s), 1566 (s), 1475 (m), 1446 (m), 1394 (s), 752 (s).

$[Mn(pic)_2]_n$ (4): A slurry composed of $MnCl_2{\cdot}4H_2O$ (0.198 g, 1.00 mmol) and picolinic acid (0.123 g, 1 mmol) in 12 mL of DMF (or CH_3OH/H_2O) was sealed into a 25-mL stainless steel reactor with a Teflon liner and heated at 145 °C for 72 h under autogenous pressure. After cooling the reactor, brown-red crystals were collected to afford 0.085 g of complex **4** with a yield of 57% based on Hpic. $C_{12}H_8MnN_2O_4$ (299.14): calcd. C 48.18, H 2.70, N 9.37, Mn 18.37; found C 48.33, H 2.76, N 9.48, Mn 18.46. IR (KBr): $\tilde{\nu}$ = 3089 (w) cm^{-1}, 3064 (w), 3020 (w), 1659 (s), 1624 (s), 1570 (m), 1408 (m), 1350 (s), 781 (m).

$[MnCl(pic)]_n$ (5): A slurry composed of $MnCl_2{\cdot}4H_2O$ (0.198 g, 1.00 mmol) and picolinic acid (0.123 g, 1 mmol) in 19 mL of MeCN (or EtOH) was sealed into a 25-mL stainless steel reactor with a Teflon liner and heated at 145 °C for 72 h under autogenous

Table 3. Crystal data, data collection and structure refinement for complexes **1**−**7**

Complex	**1**	**2**	**3**	**4**	**5**	**6**	**7**
Empirical formula	$C_{20}H_{28}N_3O_4Cl_2Mn$	$C_{12}H_{12}N_2O_6ClMn$	$C_6H_8NO_4ClMn$	$C_{12}H_8N_2O_4Mn$	$C_6H_4NO_2ClMn$	$C_6H_5Cl_2MnNO_2$	$C_{24}H_{16}N_4O_{10}Mn_2$
M	500.29	370.63	248.52	299.14	212.49	248.95	630.29
Crystal system	monoclinic	triclinic	monoclinic	monoclinic	tetragonal	monoclinic	monoclinic
Space group	$C2/c$	$P\bar{1}$	$P2_1/c$	$P2_1/c$	P4(2)/n	$C2/c$	$C2/c$
a (Å)	22.491(3)	6.7956(6)	11.8104(13)	10.4712(3)	9.7274(3)	11.956(4)	15.317(3)
b (Å)	7.4953(9)	10.6757(10)	9.9576(10)	10.9983(4)	9.7274(3)	10.403(4)	20.438(4)
c (Å)	15.837(2)	11.1699(9)	8.3149(9)	10.4124(2)	15.6894(8)	7.242(3)	9.6681(19)
α (°)	90.00	71.461(2)	90.00	90.00	90.00	90.00	90.00
β (°)	120.806(2)	83.0210(10)	100.213(2)	107.962(2)	90.00	103.463(5)	124.34(3)
γ (°)	90.00	71.960(2)	90.00	90.00	90.00	90.00	90.00
V (Å^3)	2293.1(5)	730.29(11)	962.37(18)	1140.70(6)	1484.57(10)	876.0(5)	2499.1(9)
Z	4	2	4	4	4	4	4
μ (mm^{-1})	0.839	1.117	1.630	1.168	2.077	2.070	1.077
T (K)	293(2)	293(2)	293(2)	293(2)	293(2)	293(2)	293(2)
Unique data	2010	2554	1688	1985	1309	777	2871
Observed data	1239	1648(9)	1383	1752	1038	718	2289
Refined parameters	138	199	118	172	100	61	182
R_1 [$I > 2\sigma(I)$]	0.0544	0.0534	0.0316	0.0358	0.0246	0.0254	0.0330
wR	0.1056	0.1173	0.0786	0.0924	0.0622	0.0933	0.0904

pressure. Brown crystals formed after cooling the reactor and were collected, affording 0.140 g of complex **5** with a yield of 66% based on Mn. $C_6H_4ClMnNO_2$ (212.49): calcd. C 33.92, H 1.90, N 6.59, Mn 25.85; found C 34.10, H 1.95, N 6.68, Mn 25.99. IR (KBr): $\tilde{\nu}$ = 3120 (w) cm^{-1}, 3080 (w), 1610 (s), 1587 (s), 1566 (s), 1475 (m), 1446 (m), 1396 (s), 1296 (m), 752 (s).

$[MnCl_2(4\text{-}C_5H_4NHCOO)]_n$ (6): A solution of $MnCl_2{\cdot}4H_2O$ (0.198 g, 1 mmol) in 10 mL of CH_3OH was added to a solution of isonocotinic acid (0.246 g, 2 mmol) in 20 mL of H_2O and the solution was refluxed for 14 h. After filtration the filtrate was allowed to stand for three weeks at room temperature to deposit light red crystals, which were collected, affording 0.039 g (yield 16%) of complex 7. $C_6H_5Cl_2MnNO_2$ (248.95): calcd. C 28.92, H 2.01, N 5.62, Mn 22.09; found C 30.01, H 2.36, N 5.28, Mn 21.46. IR (KBr): $\tilde{\nu}$ = 3217 (s) cm^{-1}, 1614 (vs), 1591 (s), 1495 (m), 1417 (s), 1188 (m), 764 (s), 673 (s), 428 (s).

$[Mn_2O_2(pic)_4]$ (7): Glacial acetic acid (4 mL) and picolinic acid (0.492 g, 4 mmol) were added to a solution of $Mn(CH_3COO)_2{\cdot}4H_2O$ (0.490 g, 2 mmol) in 25 mL of CH_3OH/H_2O (4:1, v/v) to give a light brown solution. After 5 minutes, $KMnO_4$ (0.087 g, 0.55 mmol) in 10 mL of water was slowly added dropwise to the solution, which was then filtered. The solvents were evaporated from the filtrate at room temperature to yield red crystals, which were separated by filtration and identified to be $Mn(pic)_3$, a known compound. The filtrate was allowed to stand to deposit black crystals, which were collected to afford 0.158 g of complex **7** with a yield of 25% based on total available Mn. $C_{24}H_{16}Mn_2N_4O_{10}$ (630.29): calcd. C 45.74, H 2.56, N 8.89, Mn 17.43; found C 45.90, H 2.62, N 8.94, Mn 17.55. This complex has been prepared by other workers.[17] Similar IR data were observed to those[10] of a complex $[Mn_2O_2(pic)_4]{\cdot}CH_3CN$ with different crystallographic data.

X-ray Crystallography: Single crystals of complexes **1**−**7** were coated with epoxy resin and mounted on a glass fiber for X-ray diffraction. Refraction data were collected on Siemens Smart CCD diffractometer with Mo-K_α radiation (λ = 0.71073 Å) at 293 K using the ω-2θ scan mode for all the complexes except for **7**, which was scanned on a Weissenberg IP diffractometer. Metal ions together with the chloride ions were first located and other non-hydrogen atoms were found in subsequent difference Fourier syntheses. Hydrogen atoms were located by geometric calculations, except those in water ligands, but their positions and thermal parameters were fixed during the structure refinement. Further crystallographic details are given in Table 3. Selected bond lengths and angles are listed in Table 1. Structure solution and refinement were carried out by standard methods using the SHELXTL-97 program package[39] on a DELL™ personal computer.

CCDC-210998 to -211004 (for **1**−**7**) contain the supplementary crystallographic data for this paper. These data can be obtained free of charge at www.ccdc.cam.ac.uk/conts/retrieving.html [or from the Cambridge Crystallographic Data Centre, 12 Union Road, Cambridge CB2 1EZ, UK; Fax: (internat.) + 44-1223-336-033; E-mail: deposit@ccdc.cam.ac.uk].

Acknowledgments

This work was supported by The State Key Basic Research and Development Plan (G1998010100), NNSFC (No. 39970177, 20273084) and the Expert Project of Key Basic Research from the Ministry of Science & Technology.

[1] O. Kahn, C. Martinez, *Science* **1998**, *279*, 44−48; O. M. Yaghi, G. M. Li, H. L. Li, *Nature* **1995**, *378*, 703−706; M. Fujita, Y. Kwon, S. Washizu, K. Ogura, *J. Am. Chem. Soc.* **1994**, *116*, 1151−1152; T. Sawaki, T. Dewa, Y. Aoyama, *J. Am. Chem. Soc.* **1998**, *120*, 8539−8540; H. A. Brison, T. P. Pollagi, T. C. Stoner, S. J. Geib, M. D. Hopkins, *Chem. Commun.* **1997**, 1263−1264; J. S. Miller, A. J. Spstein, *Chem. Commun.* **1998**, 1319−1320; C. M. Drain, F. Nafiatis, A. Vasenko, J. D. Batteas, *Angew. Chem. Int. Ed.* **1998**, *37*, 2344−2347; S. Subramanian, M. J. Zaworotko, *Angew. Chem. Int. Ed. Engl.* **1995**, *34*, 2127−2129; M. S. E. Fallah, E. Rentschler, A. Caneschi, R. Sessoli, D. Gatteschi, *Angew. Chem. Int. Ed. Engl.* **1996**, *35*, 1947−1949; C. Janiak, *Dalton Trans.* **2003**, 2781−2804.

[2] K. Wieghardt, *Angew. Chem. Int. Ed. Engl.* **1989**, *28*, 1153−1172.

[3] W. F. Beyer, I. Fridovich, *Biochemistry* **1985**, *24*, 6460−6467.

[4] W. F. Beck, G. W. Brudvig, *J. Am. Chem. Soc.* **1988**, *110*, 1517−1523.

[5] A. Zouni, H. T. Witt, J. Kern, P. Fromme, N. Krauß, W. Saenger, P. Orth, *Nature* **2001**, *409*, 739−743; J. Amesz, *Biochim. Biophys. Acta* **1983**, *726*, 1−12.

[6] V. K. Yachandra, K. Sauer, M. P. Klein, *Chem. Rev.* **1996**, *96*, 2927−2950; H. Schiller, J. Dittmer, L. Iuzzolino, W. Dörner, W. Meyer-Klaucke, V. A. Solé, H.-F. Nolting, H. Dau, *Biochem.* **1998**, *37*, 7340−7350; X.-S. Tang, B. A. Diner, B. S. Larsen, M. L. Gilchrist, G. A. Lorigan, R. D. Britt, *Proc. Natl. Acad. Sci. USA* **1994**, *91*, 704−708; A. Magnuson, L.-E. Andréasson, *Biochem.* **1997**, *36*, 3254−3261; M. L. Ghirardi, C. Preston,, M. Seibert, *Biochem.* **1998**, *37*, 17112−17119.

[7] C. W. Hoganson, G. T. Babcock, *Science* **1997**, *277*, 1953−1956; J. M. Peloquin K. A., Campbell, D. W. Randall, M. A. Evanchik, V. L. Pecoraro, W. H. Armstrong, R. D. Britt, *J. Am. Chem. Soc.* **2000**, *122*, 10926−10942; C.-X. Zhang, J. Pan, L.-B. Li, T.-Y. Kuang, *Chin. Sci. Bull.* **1999**, *44*, 2209−2215.

[8] H. Wincencjusz, H. J. Van Gorkom, C. F. Yocum, Biochem. 1997, 36, 3663−3670.

[9] M. G. Barandika, Z. E. Serna, M. K. Urtiaga, J. I. R. de Larramendi, M. I. Arriortua, R. Cortes, *Polyhedron* **1999**, *18*, 1311−1316; P. Knuuttila, *Acta Chem. Scand. Ser. A* **1982**, *36*, 767−772; Y.-Z. Li, M. Wang, L.-F. Wang, C.-G. Xia, *Acta Crystallogr.* **2000**, *C56*, e445−e446; B. N. Figgis, C. L. Raston, R. P. Sharma, A. H. White, *Aust. J. Chem.* **1978**, *31*, 2545−2548; N. Okabe, M. Koizumi, *Acta Crystallogr., Sect. C* **1998**, *54*, 288−290.

[10] E. Libby, R. J. Webb, W. E. Streib, K. Folting, J. C. Huffman, D. N. Hendrickson, G. Christou, *Inorg. Chem.* **1989**, *28*, 4037−4040.

[11] M. A. S. Goher, M. A. M. Abu-Youssef, F. A. Mautner, A. Popitsch, *Polyhedron* **1993**, *12*, 1751−1756.

[12] E. Libby, K. Folting, C. J. Huffman, J. C. Huffman, G. Christou, *Inorg. Chem.* **1993**, *32*, 2549−2556; E. Libby, K. Folting, J. C. Huffman, G. Christou, *J. Am. Chem. Soc.* **1990**, *112*, 5354−5356; E. Libby, J. K. McCusker, E. A. Schmitt, K. Folting, D. N. Hendrickson, G. Christou, *Inorg. Chem.* **1991**, *30*, 3486−3495; H. J. Eppley, S. M. J. Aubin, W. E. Streib, J. C. Bollinger, D. N. Hendrickson, G. Christou, *Inorg. Chem.* **1997**, *36*, 109−115.

[13] X. S. Tan, Z. S. Ma, N. C. Shi, D. G. Fu, J. Chen, W. X. Tang, *J. Chem. Soc., Dalton Trans.* **1996**, 2735−2739; M. A. S. Goher, M. A. M. Abu-Youssef, F. A. Mautner, A. Popitsch, *Polyhedron* **1992**, *11*, 2137−2141.

[14] X. Hao, Y.-G. Wei, Q. Liu, S.-W. Zhang, *Acta Crystallogr., Sect. C* **2000**, *56*, 296−298; H.-J. Chen, Z.-W. Mao, S. Gao, X.-M. Chen, *Chem. Commun.* **2001**, 2320−2321; W. Lin, M. E. Chapman, Z. Wang, G. T. Lee, *Inorg. Chem.* **2000**, *39*, 4169−4173; M. A. S. Goher, N. A. Al-Salem, F. A. Mautner, *J. Coord. Chem.* **1998**, *44*, 119−131; M. A. M. Abu-Youssef, A. Escuer, M. A. S. Goher, F. A. Mautner, G. J. Reiss, R. Vicente, *Angew. Chem. Int. Ed.* **2000**, *39*, 1624−1626.

[15] W. Lin, O. R. Evans, G. T. Yee, *J. Solid State Chem.* **2000**, *152*, 152−158; R. Hauptmann, M. Kondo, S. Kitagawa, *Z. Kristallogr.-New Cryst. Struct.* **2000**, *215*, 171−172; D. Xu, C. Zhang, Y. Xu, X. Huang, *Polyhedron* **1997**, *16*, 71−73.
[16] T. Matsushita, L. Spencer, D. T. Sawyer, *Inorg. Chem.* **1988**, *27*, 1167−1173.
[17] E. Larson, M. S. Lah, X. Li, J. A. Bonadies, V. L. Pecoraro, *Inorg. Chem.* **1992**, *31*, 373−378; S. P. Perlepes, A. G. Blackman, J. C. Huffman, G. Christou, *Inorg. Chem.* **1991**, *30*, 1665−1668.
[18] H. H. Thorp, *Inorg. Chem.* **1992**, *31*, 1585−1588; I. D. Brown, D. Altermatt, *Acta Crystallogr.* **1985**, *B41*, 244−247.
[19] C. Janiak, *J. Chem. Soc., Dalton Trans.* **2000**, 3885−3896.
[20] Y. C. Liang, M. C. Hong, J. C. Liu, R. Cao, *Inorg. Chim. Acta* **2002**, *328*, 152−158.
[21] B. Żurowska, J. Mroziński, *Inorg. Chim. Acta* **2003**, *342*, 23−28; M. A. S. Goher, A. K. Hafez, M. A. M. Abu-Youssef, A. Popitsch, H. P. Fritzer, F. A. Mautner, *Monatsh. Chem.* **1994**, *125*, 833−840.
[22] D.-D. Wu, T. C. W. Mak, *Inorg. Chim. Acta* **1995**, *237*, 163−167.
[23] D. F. Mullica, D. E. Pennington, J. E. Bradshaw, E. L. Sappenfield, *Inorg. Chim. Acta* **1992**, *191*, 3−6; J. Y. Lu, J. Macias, *CrystEngComm* **2002**, *4*, 17−19; Z. Wang, S. R. Wilson, B. M. Foxman, W. Lin, *Cryst. Eng.* **1999**, *2*, 91−100.
[24] N. S. Gill, R. H. Nuttall, D. E. Scaife, D. W. A. Sharp, *J. Inorg. Nucl. Chem.* **1961**, *18*, 79−87.
[25] G. B. Deacon, R. J. Phillips, *Coord. Chem. Rev.* **1980**, *33*, 227−250.
[26] R. Cortés, M. Drillon, X. Solans, L. Lezama, T. Rojo, *Inorg. Chem.* **1997**, *36*, 677−683.
[27] M. E. Fisher, *Am. J. Phys.* **1964**, *32*, 343−346.
[28] W. Hiller, J. Strähle, A. Datz, M. Hanack, W. E. Hatfield, L. W. ter Haar, P. Gütlich, *J. Am. Chem. Soc.* **1984**, *106*, 329−335.
[29] F. H. Kohler, N. Hebendanz, G. Muller, U. Thewalt, B. Kanellakopulos, R. Klenze, *Organometallics* **1987**, *6*, 115−125.
[30] J.-S. Sun, H. Zhao, X. Ouyang, R. Clerac, J. A. Smith, J. M. Clemente-Juan, C. Gomex-Garcia, E. Coronado, K. R. Dunbar, *Inorg. Chem.* **1999**, *38*, 5841−5855.
[31] B. C. Unni Nair, J. E. Sheats, R. Ponteciello, D. Van Engen, V. Petrouleas, G. C. Dismukes, *Inorg. Chem.* **1989**, *28*, 1582−1587.
[32] D. Huang, X. Zhang, C. Chen, F. Chen, Q. Liu, D. Liao, L. Li, L. Sun, *Inorg. Chim. Acta* **2003**, *353*, 284−291.
[33] Z. Sun, P. K. Gantzel, D. N. Hendrickson, *Polyhedron* **1998**, *17*, 1511−1516.
[34] O. Kahn, *Molecular Magnetism*, VCH, Weinheim, **1993**.
[35] E. Colacio, J. M. Dominguez-vera, M. Ghazi, R. Kivekäs, M. Klinga, J. M. Moreno, *Eur. J. Inorg. Chem.* **1999**, 441−445.
[36] H. Iikura, T. Nagata, *Inorg. Chem.* **1998**, *37*, 4702−4711.
[37] C. Chen, H. Zhu, D. Huang, Q. Liu, *Acta Botanica Sin.* **2000**, *42*, 1249−1252.
[38] T. Sala, M. V. Sargent, *J. Chem. Soc., Chem. Commun.* **1978**, 253−254.
[39] G. M. Sheldrick, *SHELXTL-97*, University of Göttingen, Germany, **1997**.

Received August 21, 2003
Early View Article
Published Online February 26, 2004

